Single-Particle Two-Photon Absorption Imaging and Enhancement Determination for Organic Nanoparticles

Jeffery E. Raymond and Theodore Goodson, III*

Departments of Chemistry and Macromolecular Science & Engineering, University of Michigan, 930 North University Avenue, Ann Arbor, Michigan 48109, United States

ABSTRACT The lack of characterization regimes available for the rapid single-particle assessment of two-photon (TPA) response in nanomaterials remains a critical barrier to nonlinear optical device development. This is particularly true of nonemissive species whose TPA must often be characterized in the bulk. In this study, self-assembly is used to produce uniform nanoparticles from a novel porphyrin dimer, which is known to exhibit both severe fluorescence quenching and two-photon cross section (TPACS) enhancement when assembled into macromolecules. We present here the first reported use of fiber aperture near-field optical microscopy (NSOM) for the purpose of characterizing directly the TPA of nonemissive nanoparticles, observing directly a 5-fold enhancement in TPA response. This assembly/characterization regime provides a fast and fully actualized method for the generation of low-scatter optical-limiting organic nanomaterials where domain size, morphology control, and TPA enhancement are all critical to application viability and unobservable via bulk measurements.

SECTION Nanoparticles and Nanostructures

Rapid Self Assembly

5 X Two Photon Enhancement

AFM

TPA-NSOM

Direct two photon characterization of individual non-emissive organic nanoparticles

As attempts to develop functional condensed-phase nanomaterials for nonlinear optical (NLO) applications grow more sophisticated, it is critical that methods for directly probing the NLO structure–function relationship of assemblies be actualized. This is a particularly poignant concern for developing next-generation organic nanomaterials for applications like remote sensing, light harvesting, and optical limiting.[1−3]

Directly probing the NLO character of individual nanoscale assemblies is critical to determine how subtle changes in size, morphology, and environment may enhance the response of a system. This is necessary for applications where optical-limiting or light-harvesting materials must coat or surface treat another functional device such as a CCD, remote sensor, or inorganic solar array. In these instances, it is uniformly required that the optically active coating diffract or scatter the nonabsorbed light as little as possible and generate little or no fluorescence. This can be achieved readily by using organic nanomaterials which self-assemble and have well-characterized optoelectronic properties at the interface of the particles. The viability of using two-photon excited fluorescence microscopy for probing directly the third-order nonlinear two-photon response of individual self-assembled nanomaterials has been displayed.[4−8] However, if a species experiences large quenching effects on assembly, quantitative two-photon fluorescence imaging poses a difficult prospect. This points instead to direct imaging of the multiphoton absorption. The possibility of true absorption imaging by NSOM has been displayed,[9,10] but little has been done to investigate two-photon absorption near-field imaging (TPA-NSOM) as a viable
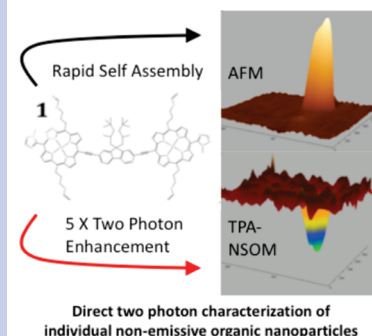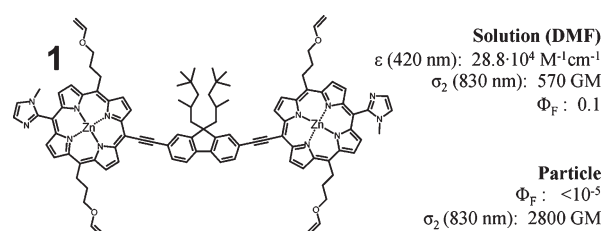
Chart 1. Porphyrin Dimer (1) and Optical Response Per Molecule

1

Solution (DMF)
ε (420 nm): $28.8\cdot10^4$ M^{-1}cm^{-1}
σ_2 (830 nm): 570 GM
Φ_F : 0.1

Particle
Φ_F : $<10^{-5}$
σ_2 (830 nm): 2800 GM

method for the quantitative inspection of nonfluorescing nanoscale materials.

Organic nanoassemblies in a variety of configurations, such as rods, macrocycles, molecular wires, ladders, and dendrimers,[4,11−14] have been shown to display enhanced NLO properties in ensemble over the individual building blocks. Previously, we have characterized an imidizoyl-terminated porphyrin dimer (Chart 1), which has be been shown to possess a TPA cross-section enhancement factor of 90 when self-assembled into a slipped cofacial macrocycle.[11] It is reasonable to assume that it is possible to assemble different architectures that capture at least some of this ensemble enhancement, even if assembly is largely with random or uncontrolled orientation.

AFM scans of the assembled nanoparticles on a mica substrate (Figure 1) show uniform porphyrin particles. The features observed in the simultaneously collected NSOM image show a
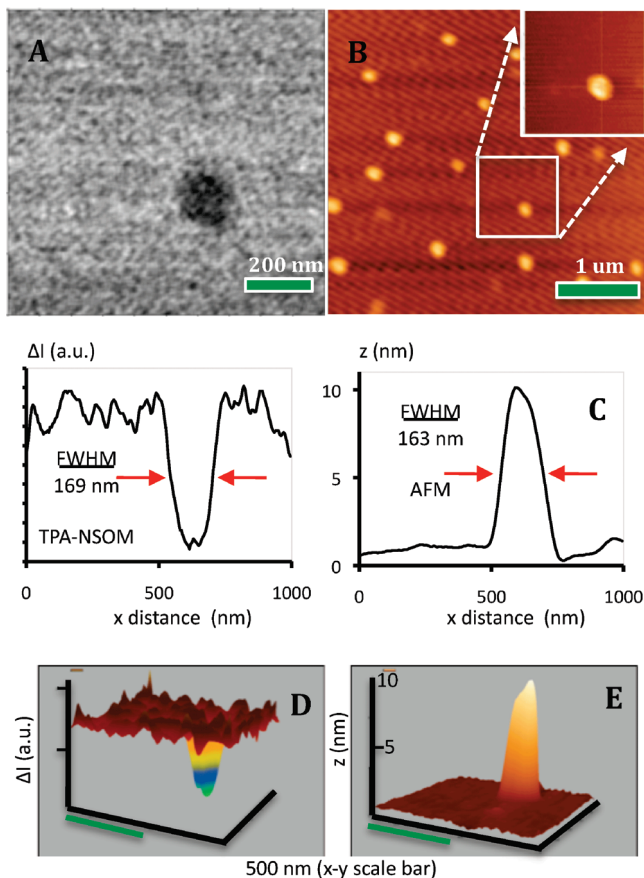
Figure 1. Topographic and near-field optical characterization of the porphyrin nanoparticle. (A) TPA-NSOM of a single particle with the contrast adjusted for maximum feature visibility using raw image data. (B) AFM of uniform particles. Single-particle image as the inset. (C) X line selections displaying feature resolution. 3D rendering of TPA-NSOM (D) and AFM (E) for a single particle. Panels C−E all use false pixel doubling and second-nearest-neighbor averaging of raw image data.

Figure 2. Power dependence determination of TPA and scattering/linear components of nanoparticle images. (A) Intensity dependence of image features including nonfeature background counts (left axis) and the change in intensity at the center of for the particle and the change in intensity without linear contributions (right axis). (B) Log−log plot confirming the I^2 dependence of the TPA contribution to ΔI by way of a slope of 2 after linear/scattering signal removal.

decrease in counts typically associated with absorption or scattering in most systems and can be imaged below an edge resolution of 15 nm. For NSOM scattering images,[15−17] this is typical of other systems with similar illumination and collection but is one of the highest reported resolutions for optical absorption images.[18,19] From peak averaging at a high incident flux, the majority contribution for this signal appears as two-photon absorption in the nanostructure and is indicated in the extracted quadratic TPA signal given in Figure 2. Quantitative polynomial extraction can be performed on the observed intensity such that

$$\iint I(x,y,i)\, \mathrm{d}x\, \mathrm{d}y = \iint s(x,y,z)I(x,y,i)\, \mathrm{d}x\, \mathrm{d}y$$
$$+ \iint t(x,y,z)I(x,y,i)^2\, \mathrm{d}x\, \mathrm{d}y \quad (1)$$

and in a pixilated environment with constant z (AFM value) and i (incident intensity), it becomes

$$\Delta I = s_z \sum_{x,y} I_{i,j} + t_z \sum_{x,y} I_{i,j}^2 \quad (2)$$

This is with s as the cofactor for scattering, t as the cofactor for TPA (linearly related to σ_2), and both s and t determined from polynomial fitting from eq 2 and shown in Figure 2.

Several scans of an individual nanoparticle were made from 21 to 168 mW of incident power on the NSOM fiber optics, having relative intensities ranging from 1 to 8 (Figure 3). Observation of the coupling efficiency for our system, through a pinhole with the probe 1 μm above contact, gives a 1.5% throughput at the probe tip due to the extremely high optical bleed at the onset of taper and spot size/rejection at the fiber coupling point. The collection efficiency for absorption imaging is presumed near 100%. Correcting for scatter, the PMT sensitivity at 830 nm, and the chromophore density, a TPACS of 2800 ± 600 GM (1 GM = 10^{-50} cm^4−s/photon) was determined for the porphyrin dimer using the following relationship, given constant incident intensity

$$\frac{(1-s)\iint I(x,y)\, \mathrm{d}x\, \mathrm{d}y}{\iint \frac{\rho}{M} N_A z(x,y)\, \mathrm{d}x\, \mathrm{d}y} = \sigma_2/\text{molecule} \quad (3)$$
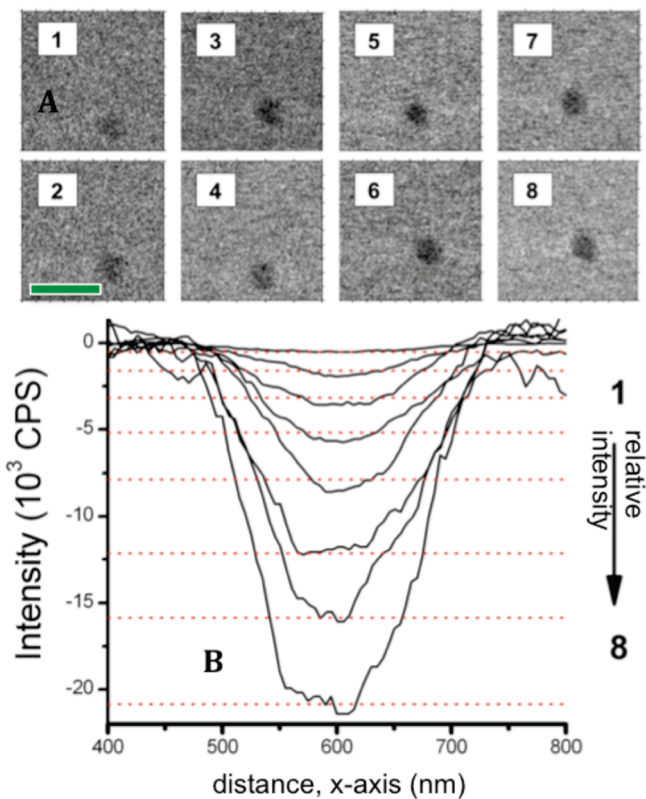
Figure 3. Power-dependent TPA-NSOM of a single porphyrin nanoparticle. (A) TPA-NSOM, relative intensities from 1 to 8. Image contrast adjusted to enhance feature visibility using raw image data. The scale bar denotes 500 nm. (B) X-axis line plots adjusted to zero background in order to provide a clear contrast of ΔI at various intensities. Red dotted lines indicate the expected change in intensity based on the signal polynomial from the fitting (eq 2) given with linear and nonlinear two-photon components.

Table 1. Summary of Experimental Results for Quantitative TPA-NSOM[a]

I_{input} (mW)	relative power	I_{obs} (10^6 cps)	N (10^3 cps)	ΔI (cps)	S/N
168	8	5.03	4.53	19166	4.23
147	7	4.43	4.51	14389	3.19
126	6	3.80	3.95	10896	2.76
105	5	3.17	3.62	6846	1.89
84	4	2.53	2.34	4339	1.86
61	3	1.83	1.86	2553	1.38
42	2	1.27	1.59	1185	0.74
21	1	0.63	1.15	305	0.26

[a] Variables: I_{input}, incident intensity coupled into fiber; I_{obs}, median nonfeature counts; N, standard deviation of nonfeature counts; ΔI, median change in intensity at the feature less the scattering/linear contribution to the counts.

than modest particle ensemble TPACS enhancement factor of 5 for this assembly method as measured by our TPA-NSOM system.

The scattering signal appears low for this system, with S/N remaining constant at ~0.2. This is specifically true when compared to other NSOM techniques in which scattering is the primary method for imaging from far-field illumination. Several components of the system, including the apertured top-down illumination, may contribute to this low observed scattering and the 830 nm wavelength. The proximity of the excitation source, low aperture diameter, $<5\,\mu$m thickness of the mica substrate, and the close proximity of the collection aperture all may result in a low observed scattering, unlike other NSOM methods in which far-field excitation and near-field collection occur and other systems where the collection is not in the direction of excitation. Additionally, far-field diffraction-type rings at $\lambda/2$ from the center of the object mass appear nominal, with intensities beginning below 1/10 of the noise level in the majority of line plots, further confirming that the majority of signal is related to near-field excitation. These features of the system lead to a series of power-dependent images by which scattering can be extracted via polynomial fitting and the two-photon character determined from the nonlinear component. Shown in Figure 3 and Table 1 are the NSOM transmission results for the study. It can be shown that the polynomial model used to determine scattering and TPA contributions reasonably matches the line scan maxima observed in Figure 3b.

Shown here for the first time is the viability of using TPA-NSOM for the observation of low-scatter systems in order to determine the exact TPA response of a nonfluorescing organic nanostructure. Through a straightforward assembly method of a known TPA material, exact per particle assessment of the NLO character can be extracted with an optical edge resolution of less than 15 nm. TPA-NSOM makes possible a high-throughput analysis of the per particle TPA for materials and their morphologies under ambient conditions even when a material's nanoscale fluorescence is difficult to observe. Through a similar, empirically rigorous regime, it can be assumed that other organic material/assembly paradigms can be investigated for low-scatter composite optical devices in the future. Additionally, in samples that do exhibit fluorescence, it

This is with ρ being an assumed density of 1.2 g/mL[20,21] and M the molar mass. The TPACS reported here is the average of three particles. From AFM, relatively uniform particle sizes were determined for this assembly method, providing heights of 9.1 ± 2 nm and diameters of 180 ± 40 nm, giving a TPACS/particle of 3.8×10^8 GM. The extremely large cross section per particle allows for greater ease of detection in contrast to comparable TPA far-field detection of single molecules like rhodamine, where cross sections are ~7−8 orders of magnitude lower. The uniform intensity assumption at the sample in this calculation may lead to some error; however, due to the near-field constraint of the fiber optic aperture, any distortion is assumed to be minimal.

In solution, this dimer possesses a TPACS of 570 GM. As a self-assembled macrocycle with 19 dimer units, the TPACS per dimer was found to be 2 orders of magnitude higher. In the macrocycle, the principle mode of enhancement was found to be related to a slipped cofacial imidizoyl−Zn association in conjunction with additional locally coordinated dimers, resulting in a greatly enhanced transition dipole coupling in the system. It is reasonable to assume, even given a random configuration, that some of the chromophores will find themselves in this or a similar environment. This leads to a more

may be possible to compare other TPEF analogue fluorescence imaging techniques[12,13] to the Z-scan analogue TPA-NSOM power dependency images, thereby clarifying discrepancies in the TPA cross sections periodically observed by comparing the two methods for solid-state materials.

EXPERIMENTAL SECTION

A femtosecond excitation source is used (Spectra-Physics Mai Tai) for this study, operated at 830 nm, 80 MHz, and a pulse fwhm of 110 fs. Intensity is regulated using a variable neutral density filter. The excitation is coupled into a CDP-NSOM multiscope with shear force AFM, absorption, and fluorescence detection capabilities. The probes use a single-mode fiber optic cable (F-SF Newport for 820 nm signaling). The probes are pretreated with weak acid to hydrolyze and soften the cladding (0.1 M HCl) and are pulled using a Sutter P-2000 CO_2 capillary puller optimized for a 13° initial taper and low-impact drawing. Tips are immediately submerged into a methanol ice bath to restrict cladding relaxation. The nominal aperture diameter is 30 nm from a nonmetalated probe, as determined from a fluorescent standard.[22] The nontrivial far- and near-field scattering signal inherent to a nonmetalated probe, which is linearly dependent on incident intensity, is removed after fitting from the nonlinear component of the feature signals. Collection is done with a 2.5 nm pixel size. False doubling to 1.25 nm and subsequent three-pixel nearest-neighbor averaging is performed on AFM and TPA-NSOM images using Nanoscope software. A 98 μM porphyrin dimer solution in 9:1 DMF/pyridine is added to Millipore purified water at a 1:20 ratio and shaken vigorously for 10 s. The resultant suspension is then vented for 30 s under a nitrogen flow and drop-deposited on cleaved mica and vacuum-dried for 30 min. Pixel size, averaging, and probe dither give a 2.5 nm uncertainty in the AFM signal $(x-y)$ and result in a nominal edge resolution in the TPA-NSOM image (5 nm) of < 15 nm.

AUTHOR INFORMATION

Corresponding Author:

*To whom correspondence should be addressed. E-mail: tgoodson@umich.edu.

REFERENCES

(1) Davis, D.; Hamilton, A.; Yang, J.; Cremar, L.; Van Gough, D.; Potisek, S.; Ong, M.; Braun, P.; Martinez, T.; White, S.; Moore, J.; Sottos, N. Force-Induced Activation of Covalent Bonds in Mechanoresponsive Polymeric Materials. *Nature* **2009**, *459*, 68–73.

(2) Hardin, B.; Hote, E.; Armstrong, P.; Yum, J.; Comte, P.; Torres, T.; Frechet, J.; Nazeeruddin, M.; Gratzel, M.; McGehee, M. Increased Light Harvesting in Dye-Sensitized Solar Cells with Energy Relay Dyes. *Nat. Photonics* **2009**, *3*, 406–410.

(3) Dini, D; Calvete, M.; Hanack, M.; Amendola, V.; Meneghetti, M. Large Two-Photon Absorption Cross Sections of Hemiporphyrazines in the Excited State: The Multiphoton Absorption Process of Hemiporphyrazines with Different Central Metals. *J. Am. Chem. Soc.* **2008**, *130*, 12290–12298.

(4) Raymond, J. E.; Ramakrishna, G.; Twieg, R.; Goodson, T. Two-Photon Enhancement in Organic Nanorods. *J. Phys. Chem. C* **2008**, *112*, 7913–7921.

(5) Hayazawa, N.; Furusawa, K.; Taguchi, A.; Kawata, S.; Abe, H. Tip-Enhanced Two-Photon Excited Fluorescence Microscopy with a Silicon Tip. *Appl. Phys. Lett.* **2009**, *94*, 193112–193114.

(6) Raymond, J. E.; Goodson, T. Quantitative Non-Linear Optical Imaging in the Nano-Regime. *Proc. SPIE* **2009**, *74130Y*, 1–7.

(7) Folling, J.; Bossi, M.; Bock, H.; Medda, R.; Wurm, C.; Hein, B.; Jakobs, S.; Eggeling, C.; Hell, S. Fluorescence Nanoscopy by Ground-State Depletion and Single-Molecule Return. *Nat. Methods* **2008**, *5*, 943–945.

(8) Hell, S. Microscopy and Its Focal Switch. *Nat. Methods* **2009**, *6*, 24–32.

(9) Knoll, B.; Keilmann, F. Near-field Probing of Vibrational Absorption for Chemical Microscopy. *Nature* **1999**, *399*, 134–137.

(10) de Paula, A.; Chaves, C.; Silva, H.; Weber, G. Absorption Coefficient Imaging by Near-Field Scanning Optical Microscopy in Bacteria. *Appl. Opt.* **2003**, *42*, 3005–3008.

(11) Raymond, J. E.; Bhaskar, A.; Makiuchi, N.; Ogawa, K.; Kobuke, Y.; Goodson, T Synthesis and Two-Photon Absorption Enhancement of Porphyrin Macrocycles. *J. Am. Chem. Soc.* **2008**, *130*, 17212–17213.

(12) Ahn, T.; Kim, K.; Kim, D.; Noh, S.; Aratani, N.; Ikeda, C.; Osuka, A.; Kim, D. Relationship between Two-Photon Absorption and the π-Conjugation Pathway in Porphyrin Arrays through Dihedral Angle Control. *J. Am. Chem. Soc.* **2006**, *128*, 1700–1704.

(13) Zheng, Q.; Gupta, S.; He, G.; Tan, L.; Prasad, P. Synthesis, Characterization, Two-Photon Absorption, and Optical Limiting Properties of Ladder-Type Oligo-*p*-phenylene-Cored Chromophores. *Adv. Funct. Mater.* **2008**, *18*, 2770–2779.

(14) Narayanan, A.; Varnavski, O.; Swager, T.; Goodson, T. Multiphoton Fluorescence Quenching of Conjugated Polymers for TNT Detection. *J. Phys. Chem. C* **2008**, *112*, 881–884.

(15) Huang, B.; Wang, W.; Bates, M.; Zhuang, X. Three-Dimensional Super-Resolution Imaging by Stochastic Optical Reconstruction Microscopy. *Science* **2008**, *319*, 810–813.

(16) Bailo, E.; Deckert, V. Tip-Enhanced Raman Scattering. *Chem. Soc. Rev.* **2008**, *37*, 921–930.

(17) McFarland, A.; Van Duyne, R. Single Silver Nanoparticles as Real-Time Optical Sensors with Zeptomole Sensitivity. *Nano Lett.* **2003**, *3*, 1057–1062.

(18) Pomraenke, R.; Ropers, C.; Renard, J.; Lienau, C.; Lur, L.; Polli, D.; Cerullo, G. Broadband Optical Near-Field Microscope for Nanoscale Absorption Spectroscopy of Organic Materials *J. Microsc.* **2008**, *229*, 197–202.

(19) Li, L.; Gattaas, R.; Gershgoren, E.; Hwang, H.; Fourkas, J. Achieving $\lambda/20$ Resolution by One-Color Initiation and Deactivation of Polymerization. *Science* **2009**, *324*, 910–913.

(20) Schauer, C.; Anderson, O.; Eaton, S.; Eaton, G. Crystal and Molecular Structure of a Six-Coordinate Zinc Porphyrin: Bis-(tetrahydrofuran)(5,10,15,20-tetraphenylporphinato) Zinc-(II). *Inorg. Chem.* **1985**, *24*, 4082–4086.

(21) LeCours, S.; DiMagno, S.; Therien, M. Exceptional Electronic Modulation of Porphyrins through *meso*-Arylethynyl Groups. Electronic Spectroscopy, Electronic Structure, and Electrochemistry of [5,15-Bis[(aryl)ethynyl]-10,20-diphenylporphinato]zinc-(II) Complexes. X-ray Crystal Structures of [5,15-Bis[(4′-fluorophenyl)ethynyl]- 10,20-diphenylporphinato]zinc(II) and

5,15-Bis[(4′-methoxyphenyl)ethynyl]-10,20-diphenylporphyrin. *J. Am. Chem. Soc.* **1996,** *118*, 11854–11864.

(22)   Kim, J.; Kim, D. C.; Nakajima, K.; Mitsui, T.; Aoki, H. Determination of the Spatial Resolution of an Aperture-Type near-Field Scanning Optical Microscope Using a Standard Sample of a Quantum-Dot-Embedded Polymer Film. *J. Korean Phys. Soc.* **2010,** *56*, 1748–1753.